Investigation of Reactivities of Bimetallic Cu-Fe Oxygen Carriers with Coal in High Temperature In-situ Gasification Chemical-Looping Combustion (iG-CLC) and Chemical-Looping with Oxygen Uncoupling (CLOU) Using a Fixed Bed Reactor

Ping Wang[a*], *Bret Howard*[a], *and Nicholas Means*[b]

[a] Department of Energy (DOE), National Energy Technology Laboratory (NETL), 626 Cochrans Mill Road, Pittsburgh, PA, 15236, USA;

[b] Leidos Research Support Team, 626 Cochrans Mill Road, P.O. Box 10940, Pittsburgh, PA 15236, USA;

*Author to whom correspondence should be addressed; E-Mail: ping.wang@netl.doe.gov; Tel.: +1-412-386-7539.

Keywords: Chemical looping, coal, Cu-based oxygen carrier, Fe-based oxygen carrier, bimetallic oxygen carrier, reactivity

ABSTRACT: Bimetallic Fe-Cu oxygen carriers (OCs) with SiO_2 as a support are attractive materials for coal chemical-looping combustion (CLC) based on their availability from naturally occurring, low cost materials. The objectives of this study are to investigate reduction reactivities and CO_2 conversion efficiency of synthesized Fe-Cu-Si OCs for both in-situ gasification CLC (iG-CLC) and Chemical-Looping with Oxygen Uncoupling (CLOU) at high temperatures (950 to 1100°C) with varying ratios of OC to coal char (ϕ) using a fixed bed reactor-quadrupole mass spectrometer system. Two Cu-Fe-Si OCs with high iron content (40% Fe_2O_3 + 20%CuO by wt.) (Fe40Cu20) and high copper content (Fe20Cu40) were prepared using a pressure pelletizing method. Oxygen uncoupling efficiency and rate for the Fe40Cu20 OC were lower than the Fe20Cu40 OC due to their $CuFe_2O_4$ and CuO composition difference from XRD analysis. For Fe40Cu20 OC with ϕ = 80 in iG-CLC, the carbon conversion rate increased 37% from 950°C to 1000°C but only increased 5.4% from 1000°C to 1100°C. As the ratios ϕ dropped (80, 40 and 24), the CO_2 conversion efficiencies decreased and the content of metallic Cu in the reduced OC residues increased. So, the optimum ratio ϕ is important to avoid agglomeration caused by Cu at high temperature. The Fe20Cu40 OC with ϕ = 67 in CLOU had higher the carbon conversion rate

($dXc/dt=0.0083\ s^{-1}$) and CO_2 conversion efficiency ($Sco_2=0.96$) compared to the Fe40Cu20 OC with $\phi = 80$ in iG-CLC ($dXc/dt=0.0037\ s^{-1}$ and $Sco_2=0.88$).

1. Introduction

Coal chemical-looping combustion (CLC) is a promising alternative technology for CO_2 capture in coal power plants because CLC generates a higher purity CO_2 product stream that minimizes the energy penalty of CO_2 capture[1, 2]. Reducing CO_2 emissions in coal power generation would have a positive effect on climate change and is critical to keep coal in the future energy mix. Research on coal CLC has been the focus of oxygen carrier (OC) studies and CLC processes during the last decade. Two main proposed processes for coal CLC are in-situ Gasification Chemical-Looping Combustion (iG-CLC) and Chemical-Looping with Oxygen Uncoupling (CLOU)[3]. Both processes have been successfully demonstrated at pilot scale in the range of 1 kWth to 1 MWth and their results proved the concept of coal CLC[2]. For iG-CLC, a 1 MWth CLC unit combusted bituminous/hard coals with Fe-based oxygen carriers made from natural ilmenite ore ($FeTiO_3$) using two interconnected circulating fluidized bed reactors (CFB) (fuel reactor and air reactor) [4-6]. The 250 kWth pilot unit of a moving bed fuel reactor coupled with a combined bubbling bed/entrained-flow air reactor was tested using synthetic Fe-based metal oxide particles with sub-bituminous and bituminous coals. Additionally, a large 10 MWe unit, including four 2.5 MWe modules, is being designed [7]. Fluidized bed fuel reactors are commonly used in solid fuel CLC tests [2] but the moving bed fuel reactor is unique and attractive due to maximizing solids conversion and maintaining complete fuel conversion [7-10]. For CLOU, Cu-based oxygen carriers (e.g. 60% CuO on a $MgAl_2O_4$ support) were tested to combust coal (e.g. lignite, bituminous, and anthracite) in a 1.5 kW CFB[11-14].

In the iG-CLC process, the coal is first gasified to produce syngas (mainly CO and H_2) under H_2O and/or CO_2 and then the syngas reacts with the OC (syngas CLC)[3]. This method is used to improve the slow solid-solid reaction of coal and the OC in the fuel reactor. Fe-based OCs in iG-CLC have mainly been investigated for coal CLC because the Fe-based OCs are relatively cheap and available from natural ores (e.g. ilmenite and iron ore) and industrial waste. Also, inexpensive OCs are preferable since OC losses may occur with coal ash that is purged out of the fuel reactor to avoid accumulation in the system [3]. From the pilot plant tests using fluidized bed fuel reactors, lowering the unburnt coal/char transferred with the OC to the air reactor and improving the CO_2 gas quality exiting the fuel reactor are still some of the major challenges [2]. To increase the CO_2 capture efficiency, research has aimed to improve the OC activity and study operating conditions like temperature and the amounts of OC and fuel present in the fuel reactor [2]. This study focuses on that goal. Additionally, proposed process improvements include the addition of a carbon stripper (separating the unburnt carbon from the OC before the air reactor), conducting an oxygen polishing step at the outlet of the fuel reactor (high concentration O_2 to oxidize the unburnt gaseous compounds), and use of a moving bed fuel reactor instead of the fluidized bed fuel reactor to increase gas-solid OC contact [2]. The pilot test, using the moving bed fuel reactor, reached near complete coal conversion (95%) and produced high purity CO_2 (~97%) [7]. However, the addition of carbon stripping and oxygen polishing steps will increase capital and operation costs.

In the CLOU process, coal is burned with gaseous oxygen released by the OC in the fuel-reactor, similar to conventional coal combustion[3]. CLOU has higher fuel conversion rates and fuel combustion efficiency compared to iG-CLC because it avoids the slow char gasification step in the iG-CLC and the fuel is combusted with gaseous oxygen[15]. Cu-based oxygen carriers have

been the focus of CLOU development because CuO has a fast oxygen release rate, high oxygen transport capacity and favorable combustion thermodynamics that completely convert fuel to CO_2 and H_2O[3, 16, 17]. CLOU with Cu-based OCs have shown high CO_2 capture efficiency and combustion efficiency without the carbon stripper used in the pilot scale tests[2]. Further materials development for CLOU to improve the OC lifetime is a still an important research area based on pilot plant tests[18].

This study investigated bimetallic copper-iron oxygen carriers (Cu-Fe OC) for coal iG-CLC and CLOU to improve the performance as compared to monometallic Fe-based and Cu-based OCs. For iG-CLC, the addition CuO to the monometallic Fe-based OC may increase the CO_2 capture efficiency due to favorable combustion thermodynamics of CuO. The phase transformations of Fe_2O_3 reduction are $Fe_2O_3 \rightarrow Fe_3O_4 \rightarrow FeO \rightarrow Fe$. When Fe_2O_3 is reduced to Fe_3O_4, it completely converts CO and H_2 to CO_2 and H_2O based on thermodynamics but it has low oxygen transport capacity (Ro=3.3%)[2]. The Ro is defined as $Ro = (m_o-m_r)/m_o$, the mass fraction of the oxygen transport between the fully oxidized m_o, and reduced m_r, oxygen carrier [3]. The phase transformations of CuO reduction are $CuO \rightarrow Cu_2O \rightarrow Cu$. CuO is reduced to Cu_2O by releasing gaseous oxygen (R1) and has higher oxygen transport capacity (Ro=10%)[3].

$$4\,CuO\,(s) \leftrightarrow 2\,Cu_2O\,(s) + O_2\,(g) \qquad (R1)$$

The additional oxygen released by CuO may increase oxygen transport capability of the monometallic Fe-based OC and allow for a lower OC:fuel ratio (ϕ) to be used. In addition, Cu_2O has a higher melting temperature 1235^{o}C than Cu 1083^{o}C[19] so iG-CLC could be operated at higher temperature. Bimetallic Cu-Fe OCs with coal iG-CLC at low temperature ($\leq$900^{o}C) were studied by Jiang et al. [20] and Yang et al. [21] and the results showed good long-term reactivity of the OCs. The OCs were prepared by mechanical mixing CuO ($\leq$ 20wt% CuO) with natural

hematite (mainly Fe_2O_3) [20] and wet impregnation of CuO (≤ 12wt% CuO) on natural hematite [21]. Jiang et al. reported that the CO_2 conversion rate for coal at 900°C was much higher than at 860, 830 and 800°C due to acceleration of coal gasification by increased reaction temperatures. This result suggests that higher temperature, above 900°C, is needed for fast coal conversion[20]. In this study, bimetallic Cu-Fe OCs with coal iG-CLC at high temperatures (950°C to 1100°C) will be investigated. The high temperature oxygen carriers may be beneficial for coal CLC processes because these higher temperatures improve the efficiency of power generation. For CLOU, addition of Fe_2O_3 to monometallic Cu-based OCs may improve the mechanical strength and reaction stability of the Cu-based OCs. Siriwardane et al. reported that the Cu-Fe OC (60% CuO, 20% Fe_2O_3 and 20% Al_2O_3 by wt.) had no agglomeration after multiple coal CLC cycles compared to pure CuO or 60% CuO/bentonite, both of which had significant agglomeration [22]. The CuO and Fe_2O_3 interreacted to form $CuFe_2O_4$. Oxygen carrier testing with coal was conducted at 800°C and the CuO in the OC was reduced to Cu. This study will investigate CLOU using Cu-Fe OC with coal at high temperature (up to1100°C). CuO will be reduced only to Cu_2O avoiding Cu which may melt at high temperature and cause agglomeration. The synergetic effects of $CuFe_2O_4$ will also be discussed.

The future of coal CLC technology development is further process scale up and industrial validation[2, 23]. Therefore, low cost OCs are in demand and studies on OC preparation using simple methods and low-cost materials are necessary. Natural Fe ore and Cu ore are relatively cheap and may be modified to make Cu-Fe OCs. These ores can have complex compositions so, to simplify analysis of the experimental results, Cu-Fe OCs were synthesized for this study using pure compounds and a simple preparation method. In this study, silicon dioxide was selected as an inert support (designated Cu-Fe-Si) because Cu-Fe-Si is commercially available and derived from

naturally occurring materials with low cost (e.g. chalcopyrite [24]). The main factors that impact the CO_2 capture efficiency are the type of OC, the temperature in the fuel reactor, the OC:fuel ratio, and the type of solid fuel[2]. Study of pure CuO reactivity in coal iG-CLC and CLOU showed that CuO oxygen uncoupling took place in both processes and the primary reactions changed with the OC:coal ratio and gas environments (such as Ar or Ar+H_2O)[19]. The objectives of this study are to investigate the reactivity and CO_2 capture efficiency of coal char with Cu-Fe OCs at high temperature (up to 1100°C) with different ratios of OC to coal char and to investigate the primary reactions taking place in iG-CLC and CLOU as well as the gas product distributions using a fixed bed reactor (FBR)-quadrupole mass spectrometer (QMS) system. The results will provide valuable information for OC development and the design and operation of chemical-looping processes at large scale.

2. Materials and methods

2.1.Coal char sample preparation and characterization

Coal char was used as the fuel sample and prepared by pyrolysis in this study. The coal was a Powder River Basin (PRB) sub-bituminous coal obtained from the U.S. Department of Energy's National Carbon Capture Center (NCCC) managed by Southern Company. The coal was first sieved to a particle size of 106-180 μm to avoid mass and heat transfer limitations during the char reaction. Pyrolysis was conducted in a preheated fixed bed reactor at 1000^{o}C for 1 hr under flowing nitrogen to remove volatiles in the coal. Table 1 lists the proximate and ultimate analysis results of the coal and the coal char on a dry basis[19]. The moisture content of the char and coal were 1.20 wt% and 12.29 wt%, respectively.

Table 1. Proximate and ultimate analysis of the Powder River basin (PRB) sub-bituminous coal and char[19].

Sample	Proximate analysis (% dry basis)			Ultimate analysis (% dry basis)				
	Fixed carbon	Volatile matter	Ash	C	H	N	S	O (diff.)
PRB Char	85.60	1.98	12.42	85.60	0.23	1.12	0.53	0.10
PRB Coal	47.66	45.08	7.26	65.44	4.39	0.72	0.48	21.71

2.2.Bimetallic Cu-Fe-Si OCs preparations and characterization

Bimetallic Cu-Fe OCs were synthesized using mechanical mixing followed by pressure pelletizing [25-27]. The starting materials were active metal oxides of cupric oxide (CuO) (powder, 99.99% trace metals) and ferric oxide (Fe_2O_3) (powder, 99% assay) with an inert silicon dioxide support (SiO_2) (analytical reagent, quartz from XRD analysis) from Sigma-Aldrich. The SiO_2 support was used to inhibit the OCs fast deactivation via agglomeration and improve the mechanical stability (e.g. attrition).

A mixture containing 60 wt.% CuO and Fe_2O_3 with 40 wt.% SiO_2 support was prepared. A water slurry was formed by adding distilled water to the mixture and stirring intensively. The slurry was dried at 110^{o}C in an oven under N_2 to obtain a suitable mixture for pelletization. Cylindrical pellets (13mm in diameter and 3mm high) were pressed (pressing pressure ~10,000kg) in a laboratory hydraulic press. The pellets were calcined at high temperature (1000˚C or 1100^{o}C) under flowing air in a furnace for 2 hours in order to enhance OC mechanical resistance. After calcination, the pellets were ground with a mortar and pestle and sieved till particle sizes less than 180 µm. The particle sizes of the OCs (Fe60, Fe40Cu20 and Fe20Cu40) were small and similar with an average particle size of about 100 µm from sieve analysis (90, 106, 125, 150, and 180 µm screens).

The Cu-Fe OCs with four different ratios of CuO to Fe_2O_3 (20/40, 40/20, 50/10 and 60/0 wt. %) were prepared. The Cu-Fe OCs that contained high CuO content (50 and 60 wt.%) exhibited

significant sintering at both calcination temperatures; 1000 and 1100˚C. Sintering was also observed for the Cu40 (40% CuO, 20% Fe_2O_3 and 40% SiO_2) OC calcined at 1100˚C. Adanez et al. also reported the sintering problem for OCs containing ≥ 40wt% CuO with a SiO_2 support prepared using a similar method and calcinated at ≥ 1100˚C[28]. Because of this, two Cu-Fe OCs were prepared and calcined at 1000ºC: Fe40Cu20 (40% Fe_2O_3, 20% CuO and 40% SiO_2) and Fe20Cu40 (Table 2). A reference OC, Fe60 (60% Fe_2O_3 and 40% SiO_2), was also prepared by the same method as the Cu-Fe OCs to study the impact of CuO addition on the Cu-Fe OC reactivity (Table 2).

Table 2. Types of Cu-Fe oxygen carriers, related process, its chemical compositions in preparation and main active phase compounds in fresh prepared OCs from XRD analysis.

OC Name	**Process**	**Concentration (wt.%)**			**Main active phases**
		CuO	**Fe_2O_3**	**SiO_2**	
Fe60 (reference)	iG-CLC	0	60	40	Fe_2O_3 (hematite)
Fe40Cu20	iG-CLC	20	40	40	$CuFe_2O_4$ (tetragonal, cubic) CuO (trace)
Fe20Cu40	CLOU	40	20	40	CuO $CuFe_2O_4$ (tetragonal, cubic)

For the Fe40Cu20 OC, the molar ratio of CuO to Fe_2O_3 was 1:1. During the calcination process, CuO reacted with Fe_2O_3 forming copper ferrite ($CuFe_2O_4$). The reaction could be described by R2 [20, 29].

$$CuO\ (s) + Fe_2O_3\ (s) \rightarrow CuFe_2O_4\ (CuOFe_2O_3)\ (s) \qquad (R2)$$

The X-ray diffraction (XRD) results of the Fe40Cu20 OC showed that the active phase was mainly $CuFe_2O_4$ (mixture of tetragonal and cubic) with trace amount of CuO (Table 2). This was in agreement with phase equilibria as a function of oxygen partial pressure in the system for Cu-Fe-

O at 1000°C [30, 31]. For the Fe40Cu20 OC, which contained a metal mole fraction $n_{Fe}/(n_{Fe}+n_{Cu})$ = 0.67, in air (21% O_2) the stable compounds were spinel $Cu_xFe_{3-x}O_4$ (X=1) + CuO and/or Fe_2O_3. This occurred because the composition was close to the line dividing the two phases of $Cu_xFe_{3-x}O_4$ (X=1) + CuO and $Cu_xFe_{3-x}O_4$ (X=1) + Fe_2O_3. Ristić et al. studied the solid state reaction between CuO and α- Fe_2O_3 at the initial molar ratio of 1:1 at 800, 1000 and 1100°C for 1hr [32]. They found that the products at 1000°C contained mostly cuprospinel ($CuFe_2O_4$, cubic) with a trace amount of tenorite (CuO). The Fe40Cu20 OC phase composition was mostly in agreement with their results.

For the Fe20Cu40 OC, the molar ratio of CuO to Fe_2O_3 was 4:1. A portion of the CuO reacted with Fe_2O_3 and formed $CuFe_2O_4$ according to R2 but the remaining CuO was a separate phase. The active phase of Fe20Cu40 OC was mainly CuO and $CuFe_2O_4$ (tetragonal and cubic) from the XRD analysis (Table 2). This was in agreement with phase equilibria as a function of oxygen partial pressure for Cu-Fe-O at 1000°C [30, 31]. For the Fe20Cu40 OC, which contained a metal mole fraction $n_{Fe}/(n_{Fe}+n_{Cu})$ = 0.2, in air (21% O_2) the stable compounds were spinel $Cu_xFe_{3-x}O_4$ (X=1) + CuO. The reference Fe60 OC consisted of Fe_2O_3 (hematite) from the XRD analysis (Table 2).

2.3. Experimental set-up and analysis of the Cu-Fe OCs

A schematic of the FBR--QMS (Pfeiffer Ominstar GSD 301) system used in this study is shown in Figure 1. The quartz reactor tube had a 22 mm I.D. and a length of about 600 mm. The reactor tube was positioned inside a horizontal tube furnace (ThermoScientific Lindberg/Blue M

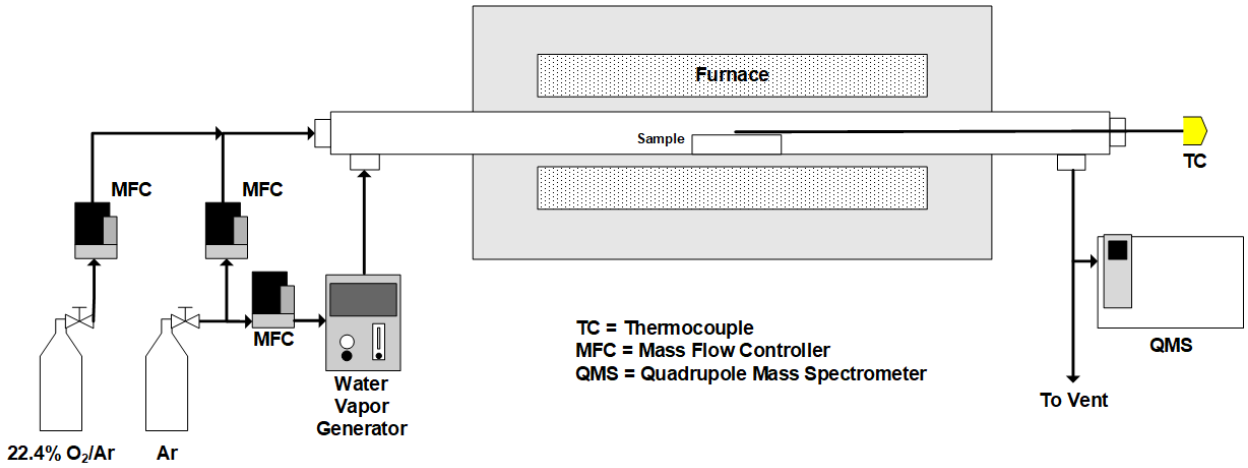

Figure 1. Schematic of the experimental FBR-QMS setup used in this study.

TF55030A-1). The test sample (for example10 mg char + 800 mg OC) was placed into a CoorTek porcelain combustion boat in the middle of the tube. The sample was a thin layer at the bottom of the boat (70 mm L x 14 mm W x 10 mm H with a 2 mm wall thickness) to reduce mass and heat transfer resistances. The length of the particle bed was about 66 mm. The loaded system was purged with Ar to remove air and monitored by the QMS. For reduction in the Ar+H_2O environment (iG-CLC), the gases, Ar or 22.4% O_2/Ar were fed to the FBR at ~120 ml/min by mass flow controllers (MFCs) for the purging or oxidization. Water vapor (H_2O+Ar), from another gas line, was fed to the system after the sample was preheated to 200^{o}C. Preheating was done to avoid water condensation in the cold sample and to shorten the heating time to the desired final test temperature. The water vapor was produced using a water vapor/relative humidity generator (L&C Science and Technology HG-100), in which Ar (~50ml/min by the MFC) flowed through a heated water tank at 80^{o}C. To prevent water condensation in the transfer line, a line heater was used to maintain a temperature of 165^{o}C. The total gas flow of Ar+H_2O in the reactor was 170 ml/min. For the reduction in Ar environment (CLOU), the Ar flow was ~170 ml/min. The superficial gas velocity of the reactor was ~7.5 mm/s and gas solid contact time was ~8.8 s. Following that, the

sample was heated to the final test temperature at a heating rate of ~65°C/min and then held until the reaction finished. The test temperature was measured using a K-type thermocouple placed next to the sample. The sample was placed in the constant temperature range of the tube furnace. The gas flow rates and test temperatures were recorded every second using LabVIEW software. The product gas compositions were analyzed on-line by QMS at one second intervals until the reaction ceased. The QMS was calibrated to quantitatively measure ~~of~~ Ar, CO, CO_2, CH_4, H_2, and H_2O. The crystalline phase composition of solid residue remaining after each test was analyzed using XRD (PANalytical X'Pert PRO).

To understand the reactions taking place in coal CLC with the Cu-Fe OCs (OC oxygen uncoupling, OC reduction with char and OC re-oxidation in iG-CLC and CLOU), test conditions such as temperature, OC/char ratio (ϕ) and gas environment (Ar or Ar+H_2O) were investigated. The uncoupling properties of the Fe40Cu20 and Fe20Cu40 OCs (approximately 0.2g) were tested under Ar at 1000˚C (Table 3). For the Fe40Cu20 OC, iG-CLC was considered based on the low oxygen uncoupling of the OC. The Fe40Cu20 OC with char at ϕ = 80 was tested under Ar+H_2O for reduction and 22.4%O_2/Ar for re-oxidation. The OC/char ratio ϕ = 80 was selected assuming the CuO and Fe_2O_3 added in the OC were ideally reduced to Cu_2O (R3) and Fe_3O_4 (R4), respectively.

$$4CuO + C\ (s) \rightarrow 2Cu_2O + CO_2\ (g) \qquad (R3)$$

$$6Fe_2O_3 + C\ (s) \rightarrow 4Fe_3O_4 + CO_2\ (g) \qquad (R4)$$

To understand the addition of CuO on Fe-based iG-CLC, Fe60 OC with char at ϕ = 135 was tested at 950˚C. Assuming the Fe_2O_3 added in the OC was ideally reduced to Fe_3O_4, an OC/char ϕ =114 (R4) was required. The higher OC/char ratio ϕ = 135 was selected to maximum char to CO_2 conversion. The influence of temperature on the OC reduction activity with char at

ϕ =80 was investigated at 950, 1000 and 1100˚C. Char gasification was also studied at these conditions because gasification is the controlling step for reduction in iG-CLC. Char gasification was conducted at the ratio of char to SiO_2 of 80 (char/SiO_2 = 80) to be comparable to the OC with char tests. The impact of OC/char ratio (ϕ = 80, 40 and 24) on the reaction reactivities was also studied.

For the Fe20Cu40 OC, CLOU was considered based on the high oxygen uncoupling of the OC. The ratio of OC to coal ϕ = 67 was selected assuming CuO added in the OC was ideally reduced to Cu_2O (R3). The Fe20Cu40 OC with char at ϕ =67 was tested at 1000˚C under Ar for reduction and 22.4%O_2/Ar for re-oxidation. A similar test was also done using Ar+H_2O to study the influence of water on the reactivity of the OC with char in CLOU to simulate steam as the fluidizing gas. The impact of OC/char ratio on the reactivities were investigated at ϕ = 67 and 18 under Ar+H_2O.

2.4. Data analysis

For the Cu-Fe OC oxygen uncoupling, the CuO alone or in $CuFe_2O_4$ ($CuOFe_2O_3$) released gaseous O_2 and reduced to cuprous oxide (Cu_2O) upon heating. This is explained in section 3.1. The OC uncoupling reactivity was quantified in terms of oxygen uncoupling, Xo and oxygen uncoupling rate, dXo/dt. Xo was calculated as:

$$Xo = \frac{n}{n_{max}} \quad (1)$$

where n is the moles of accumulated gaseous oxygen generated over the reaction time (t) and n_{max} is the moles of the gaseous oxygen generated from the CuO in the OC for the Fe40Cu20 and Fe20Cu40 OCs and calculated based on the reaction R1. In addition, the OC oxygen transport capacity by oxygen uncoupling (Roc = m_{o2}/m_c) was also calculated from the total amount of

generated gaseous O_2 measured using QMS m_{o2} over the initial mass of the OC m_c. It was derived from the traditional oxygen transport capability Ro.

During CLOU and iG-CLC in the fuel reactor, the char was converted by the OC reduction and primarily generated CO_2, CO, H_2 and H_2O. The reactivities were quantified in term of the carbon conversion efficiency (Xc) and carbon conversion rate, dXc/dt. Xc was defined as:

$$Xc = \frac{n_c}{n_0} = \frac{\sum_{t=0}^{t} F(y_{CO2}+y_{CO})}{n_0} \quad (2)$$

where n_c is the moles of accumulated carbon in carbon containing product gases over the reaction time (t). This was calculated based on the volumetric concentrations of the carbon containing gases CO_2 and CO (y_i) and the gas flow rate (F). The parameter n_o is the moles of the carbon in the initial coal char sample and calculated based on the char proximate and ultimate analyst results (Table 1).

The goals of coal CLC are to completely convert coal to CO_2 and H_2O in the fuel reactor and to fully capture CO_2 after H_2O condensation in coal power plants. The CLC performance of OC reduction with coal was quantified in terms of the CO_2 conversion efficiency (Sco_2)[24]. Sco_2 is defined as:

$$Sco_2 = \frac{n_{CO2}}{n_t} \quad (3)$$

where n_{CO_2} and n_t are the total moles of accumulated carbon in CO_2 and in carbon containing gases (CO_2 and CO) in the outlet stream during the test, respectively.

3. Results and discussion

3.1. Oxygen uncoupling of Fe40Cu20 OC and Fe20Cu40 OC

In the oxygen uncoupling tests of Fe40Cu20 OC and Fe20Cu40 OC, gaseous O_2 was generated (above 738°C for the Fe40Cu20 OC and 832°C for the Fe20Cu40 OC) and detected by the QMS in the product gas. Figure 2 shows the oxygen uncoupling (Xo), oxygen uncoupling rates

(dXo/dt) and measured sample temperatures of the Fe40Cu20 OC and Fe20Cu40 OC. For the Fe40Cu20 OC, the final oxygen uncoupling was Xo = 0.78 (Table 3), which meant that part of the CuO added during the Fe40Cu20 OC preparation was decomposed to Cu_2O and released O_2 based on the Xo definition (Equation 1). The oxygen uncoupling curve had one peak with the maximum oxygen uncoupling rate dXo/dt = 0.0031 s^{-1} at the temperature Tmax = 960^{o}C.

The oxygen uncoupling behavior of the Fe20Cu40 OC was different than the Fe40Cu20 OC. Most of the CuO added in the Fe20Cu40 OC preparation was converted with the final oxygen uncoupling Xo = 0.98 (Table 3). The maximum oxygen uncoupling rate of the Fe20Cu40 OC was dXo/dt = 0.0077 s^{-1} at the temperature Tmax = 975^{o}C. This was 2.5 times faster than the Fe40Cu20 OC. Compared to the oxygen uncoupling of pure CuO, measured with a similar method at 850 (dXo/dt = 0.0015 s^{-1}) and 950^{o}C (dXo/dt = 0.0077 s^{-1}) [19], the Fe20Cu40 OC results were similar to CuO at 950^{o}C (Table 4). From the uncoupling tests, $CuFe_2O_4$ released less gaseous O_2 than CuO, which was in agreement with the results from the Cu-ore (containing CuO and $CuFe_2O_4$) study [33]. Overall, the different compositions of the Fe40Cu20 and Fe20Cu40 OCs and the oxygen uncoupling behaviors of active compounds (CuO and $CuFe_2O_4$) are all reasons for the higher Xo and dXo/dt of Fe20Cu40 OC compared to Fe40Cu20 OC.

The maximum temperatures for the Fe40Cu20 OC and Fe20Cu40 OC were different because the Fe20Cu40 OC was heated more quickly to 1000^{o}C than the Fe40Cu20 OC due to differences in their heat capacity (Figure 2). The molar heat capacity of $CuFe_2O_4$ in the Fe40Cu20 OC was 205.62 J/(mol K) and this was 3.5 times higher than CuO (58.10 J/(mol K)), the main component of the Fe20Cu40 OC. These values were estimated using HSC Chemistry 9 software.

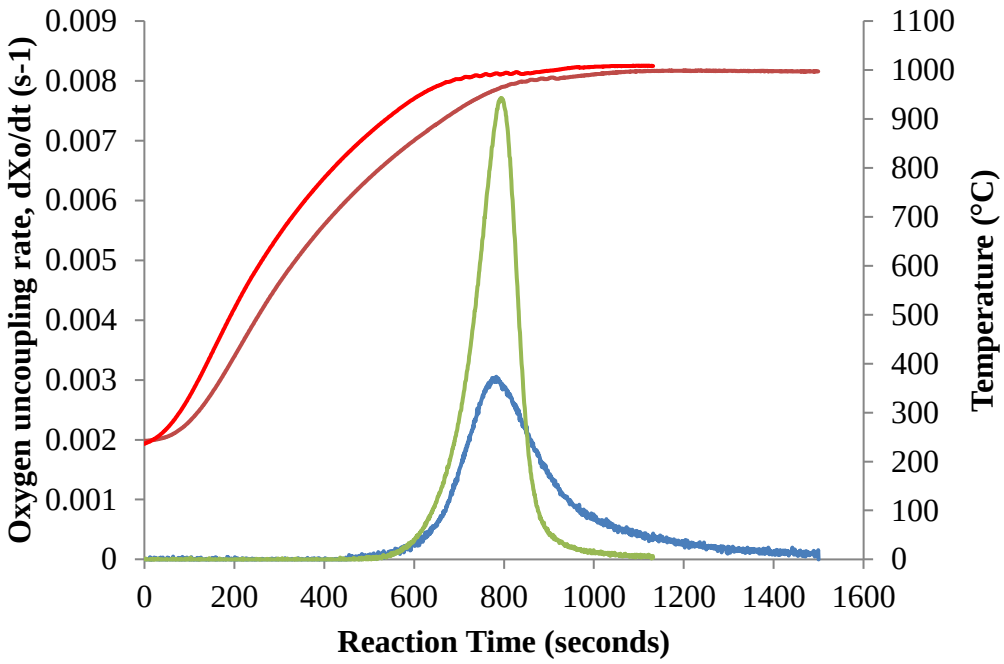

1

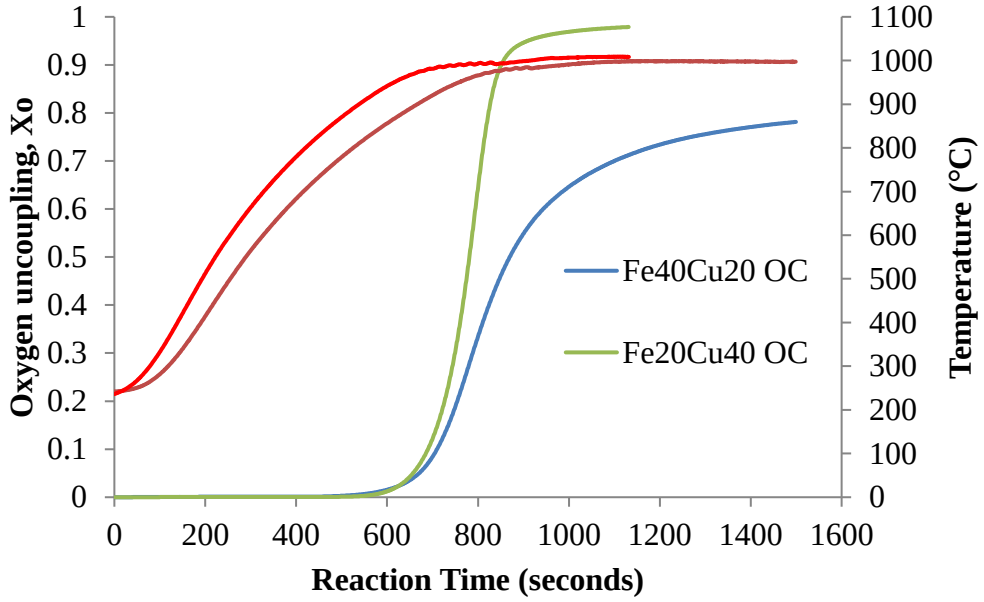

2

3 Figure 2. The reaction temperatures, oxygen uncoupling (Xo) (a) and oxygen uncoupling rates

4 (dXo/dt) (b) vs. time of Fe40Cu20 OC and Fe20Cu40 OC at 1000°C in Ar.

Table 3. Oxygen transport capacity Roc, final oxygen uncoupling Xo, maximum oxygen uncoupling rates dXo/dt, temperatures, and main active phases of the uncoupled OCs from XRD analysis for Fe40Cu20 and Fe20Cu40 OCs in Ar at 1000 °C and CuO* (*from reference[19]).

Type of OC	**T (°C)**	**Oxygen uncoupling reactivities**				**Main active phases in uncoupled OCs from XRD analysis**
		Roc	**Xo**	**Tmax (°C)**	**dXo/dt (s^{-1})**	
Fe40Cu20 OC	1000	0.016	0.78	960	0.0031	$CuFeO_2$ (rhombohedral) $Cu_xFe_{3-x}O_4$ (x=0.67, cubic)
Fe20Cu40 OC	1000	0.040	0.98	975	0.0077	Cu_2O (cuprite) $CuFeO_2$ (rhombohedral)
CuO*	850	0.10	1.0	850	0.0015	Cu_2O (cuprite)
	950	0.10	1.0	922	0.0077	Cu_2O (cuprite)

XRD results indicated that $CuFeO_2$ (rhombohedral) and $Cu_xFe_{3-x}O_4$ (x =0.67) (cubic) were generated without Fe_2O_3 in the residue of the Fe40Cu20 OC uncoupling tests (Table 3). This agreed with the phase equilibria as a function of oxygen partial pressure in the Cu-Fe-O system at 1000°C [30, 31]. For the Fe40Cu20 OC, with $n_{Fe}/(n_{Fe}+n_{Cu}) = 0.67$ at the maximum O_2 pressures $P_{O2} = 0.00084$ atm, the stable compounds were $CuFeO_2$ and $Cu_xFe_{(3-x)}O_4$. This was different than reported for $CuFe_2O_4$ uncoupling at lower temperatures ≤ 900°C [24, 34]. $CuFe_2O_4$ released O_2 and generated $CuFeO_2$ and Fe_2O_3 (Reaction R5). This also indicated that CuO in the $CuFe_2O_4$ ($CuOFe_2O_3$) mainly released gaseous O_2 and reduced to cuprous oxide (Cu_2O) in $CuFeO_2$ ($Cu_2OFe_2O_3$). The reason for this difference is because the phase equilibria of the Cu-Fe-O system is also impacted by temperature along with the oxygen partial pressure [35]. At an O_2 pressure of

$$2CuFe_2O_4\ (CuOFe_2O_3)\ (s) \leftrightarrow 2CuFeO_2\ (Cu_2OFe_2O_3)\ (s) + Fe_2O_3\ (s) + 1/2O_2\ (g) \quad (R5)$$

0.01 atm, the stable compounds $Fe_2O_3 + Cu_xFe_{(3-x)}O_4$ at low temperatures (≤ 1080°C) changed to $Cu_xFe_{(3-x)}O_4$ at high temperature. Therefore, the $CuFe_2O_4$ uncoupling at high temperature released

gaseous O_2 and reduced to $CuFeO_2$ (rhombohedral) and $Cu_xFe_{3-x}O_4$ (x =0.67) (cubic). This was further confirmed by XRD analysis of the Fe20Cu40 OC uncoupling residue that mainly contained Cu_2O from CuO, $CuFeO_2$ (rhombohedral) and $Cu_xFe_{3-x}O_4$ (x =0.67) (cubic) from $CuFe_2O_4$ (Table 3).

The major active compounds of the Fe20Cu40 and Fe40Cu20 OCs were CuO and/or $CuFe_2O_4$ (Table 2). CuO released gaseous O_2 and was reduced to Cu_2O during heating (Reaction R1)[15]. The oxygen transport capacity of pure CuO from oxygen uncoupling is Ro = 0.1 based on simple stoichiometric calculations (R1) [3]. The Roc of Fe40Cu20 OC, calculated from the uncoupling test, was 0.016 and this was lower than the ideal Ro = 0.02 based on 20% CuO added during the OC preparation (Table 2). This occurred because $CuFe_2O_4$ ($CuOFe_2O_3$) was formed from the CuO and Fe_2O_3 reaction (R2) and only part of the CuO in $CuFe_2O_4$ was reduced to Cu_2O (Table 3). The Roc of Fe20Cu40 OC, calculated from the uncoupling test, was 0.040 which was close to the ideal Ro = 0.04 based on 40% CuO added in the OC preparation (Table 2). These values were in better agreement because CuO was the major active compound in the OC (Table 3).

3.2. Fe40Cu20 OC with Coal Char in iG-CLC

3.2.1. Reactivities and possible reactions of the Fe40Cu20 OC and char during iG-CLC

The reactivity of the Fe40Cu20 OC with the char at $\phi = 80$ was tested at 1000°C in Ar+H_2O. The product gas was mainly CO_2 with small amounts of CO and H_2 (Figure 3). The final carbon conversion efficiency of the char was Xc=0.96 (Table 4). This was close to the theoretical carbon conversion efficiency ($X_{c\ theo}$=1) and indicated that the chars were nearly completely converted. The carbon conversion curve had one peak with the maximum carbon conversion rate dXc/dt = 0.0039 s^{-1} at the temperature Tmax = 956°C.

Table 4. Final carbon conversion efficiencies, CO_2 conversion efficiencies, maximum conversion rates and temperatures for the Fe40Cu20 OC with char at ϕ = 80 and char/SiO_2 in Ar+H_2O at 950, 1000 and 1100°C.

Sample	T (°C)	Carbon conversion in reduction Xc	Sco_2	R_{max} (s^{-1})	T_{max}(°C)	Main active phases in reduced OCs from XRD analysis
Fe60 OC/char ϕ = 135	950	0.99	0.78	0.0031	935	Fe_3O_4 (magnetite) Fe_2O_3 (hematite)
Fe40Cu20 OC/char ϕ = 80	950	0.94	0.82	0.0027	930	$Cu_xFe_{3-x}O_4$ (x=0.67) $CuFeO_2$ Cu (trace)
	1000	0.96	0.88	0.0037	966	
	1100	0.99	0.69	0.0039	972	
SiO_2/char	950	0.94	0.65	0.0025	950	
	1000	0.99	0.54	0.0036	986	
	1100	0.97	0.47	0.0040	1026	

To understand the reaction of the Fe40Cu20 OC with char, char gasification with SiO_2 only (same ratio as used with OC experiments) was tested. Figure 3 shows the gas concentrations versus carbon conversions for (a) the char reactions with Fe40Cu20 OC at ϕ = 80 and (b) char gasification at 1000°C in Ar+H_2O. The CO_2 conversion efficiency Sco_2 = 0.88 of the Fe40Cu20 OC was higher than the char gasification, Sco_2=0.54 (Table 4). The char gasification generated syngas consisting primarily of H_2, CO and CO_2 (Figure 3) through the possible reactions: water gas reaction (R6), Boudouard reaction (R7) and water gas shift reaction (R8)[36]. In the reaction of the Fe40Cu20 OC with char, H_2 and CO from gasification might react with the active phase $CuFe_2O_4$ in the Fe40Cu20 OC and convert to H_2O and CO_2.

Water gas reaction $C(s) + H_2O \Leftrightarrow CO + H_2$ +131 MJ/kmol (R6)

Boudouard reaction $C(s) + CO_2 \Leftrightarrow 2CO$ +172 MJ/kmol (R7)

Water gas shift reaction $CO + H_2O \Leftrightarrow CO_2 + H_2$ -41 MJ/kmol (R8)

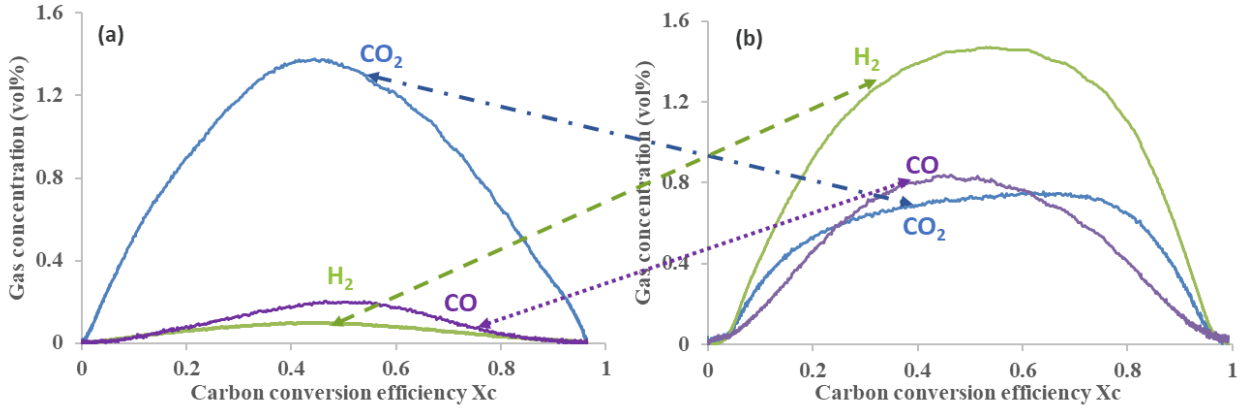

Figure 3. The gas concentrations vs carbon conversions for (a) the char reactions with Fe40Cu20 OC at ϕ = 80 and (b) the char gasification with SiO_2 (same amount as the OC) at 1000°C in $Ar+H_2O$.

The Fe40Cu20 OC released gaseous O_2 from the OC oxygen uncoupling test in section 3.1. The char reacted with the O_2 to produce CO_2, similar to conventional combustion. The uncoupling/combustion reactions mainly occurred at the beginning of the OC reduction with char (Figure 3). This may have occurred because the Fe40Cu20 OC oxygen uncoupling took place at a lower temperature (Tmax=960°C) than the char gasification (Tmax=986°C). Figure 3 (a) also showed higher CO_2 concentration at low Xc (Xc <0.1) during reduction compared to the total amount of CO_2 and CO (if it was converted to CO_2) from char gasification (Figure 3 (b)). A study of pure CuO with coal char, tested in $Ar+H_2O$ at 950°C, also reported that uncoupling/combustion was the main reaction at beginning of the test instead of gasification/syngas reduction[19]. At the same time, CO and H_2 from char gasification may react with the O_2 to produce CO_2 and H_2O. Based on the oxygen transport capacity of the Fe40Cu20 OC from oxygen uncoupling (Roc =

0.016), the released O_2 ideally combusts 57% of the char to CO_2 at ϕ = 80. Therefore, char combustion, char gasification and syngas reduction took place with the Fe40Cu20 OC and char.

From XRD analysis, the residue of the Fe40Cu20 OC and char at ϕ = 80 contained mainly $CuFeO_2$ (rhombohedral) and $Cu_xFe_{3-x}O_4$ (x =0.67) (cubic) with trace amounts of Cu (Table 4). The primary phases, $CuFeO_2$ and $Cu_xFe_{3-x}O_4$ (x =0.67), were the same as the uncoupling test (Table 3). This was expected but the amounts might not be the same. Quantitative estimates were not attempted due to the complexity of the XRD patterns. The trace Cu present in the sample might be generated from the CuO in the fresh Fe40Cu20 OC. After re-oxidation of the reduced Fe40Cu20 OC in 22.4%O_2/Ar, the phases present were $CuFe_2O_4$ (tetragonal, cubic) with trace CuO. This was the same as the fresh Fe40Cu20 OC (Table 2). So, after one cycle, the Fe40Cu20 OC did not change its phases and may be used for multiple cycles. This will be investigated in the future.

3.2.2. Addition of CuO in Fe-based OC: influences on the reactivities of Fe-based OC and coal char iG-CLC

To study the impact of CuO addition on Fe-based OC reactivity with char, the Fe40Cu20 OC with coal char at ϕ = 80 and the Fe60 OC at ϕ = 135 were tested at 950^{o}C in Ar+H_2O. Product gases from both tests were mainly CO_2 with small amounts of CO and H_2 (Figure 4). The CO_2

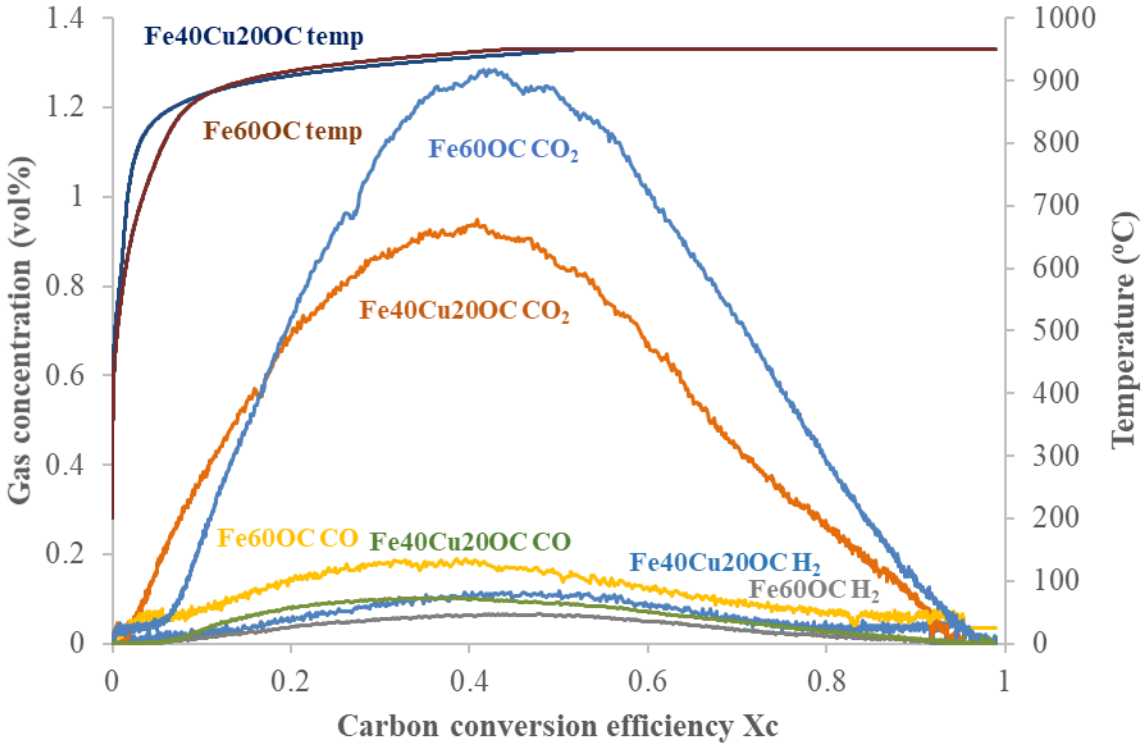

Figure 4. The gas concentrations vs carbon conversions for the reactions of coal char with the Fe40Cu20 OC at ϕ = 80 and the Fe60OC at ϕ = 135 at 950°C in Ar+H_2O.

conversion efficiency of the Fe40Cu20 OC Sco_2=0.83 was higher than the Fe60 OC Sco_2=0.78 (Table 4). In the Fe60 OC with char, char gasification and syngas reduction took place similar to Fe40Cu20 OC with char but without carbon combustion. Based on thermal analysis of Fe_2O_3 reduction using CO and H_2 as fuels at 800 and 1000°C, only Fe_2O_3 to Fe_3O_4 may completely combust CO and H_2 to CO_2 and H_2O (R9). Further reduction to FeO or Fe would increase CO and H_2 equilibrium concentrations in the outlet gas from the fuel reactor[37]. In this study, ϕ = 135

$$6Fe_2O_3 + CO\ (g) + H_2\ (g) \rightarrow 4Fe_3O_4 + CO_2\ (g) + H_2O\ (g) \qquad (R9)$$

was higher than the value required to reduce Fe_2O_3 to Fe_3O_4 (ϕ = 114) but the product gas still had not completely converted CO and H_2 during the test (Figure 4). At this OC/char ratio (ϕ), the Fe_2O_3

could combust more carbon than the carbon present in the char during the test. As a result, the char should be completely converted by the excess Fe_2O_3 in the test. XRD analysis indicated that the test residues contained Fe_3O_4 (magnetite) with some unconverted Fe_2O_3 (hematite), as expected (Table 4). The addition of CuO to the Fe-based OC slightly increased CO_2 conversion efficiency and reduced CO and H_2 in the product gas.

The final carbon conversion efficiencies of the Fe40Cu20 OC (Xc=0.94) and Fe60 OC (Xc=0.99) were similar (Table 4). The maximum carbon conversion rate of Fe40Cu20 OC dXc/dt = 0.0027 s^{-1} at the temperature Tmax = 930°C was slightly lower than Fe60 OC dXc/dt = 0.0031 s^{-1} at Tmax = 935°C. This may be due to the char combustion at the beginning of the Fe40Cu20 OC and char reaction. It resulted in less char in the following char gasification/syngas reduction of Fe40Cu20 OC with char compared to Fe60 OC with char. The rate of Fe_2O_3 being reduced to Fe_3O_4 by CO increased with increasing CO concentration[38].

3.2.3. Impact of reaction temperatures on the reactivity of Fe40Cu20 OC and coal char

To study the impact of reaction temperatures on the Fe40Cu20 OC reactivity with coal char, the Fe40Cu20 OC was tested at ϕ = 80 and 950, 1000 and 1100°C in Ar+H_2O. Char gasification with SiO_2 (same ratio as used with OC experiments) was also performed at the same conditions because char gasification is the controlling step in iG-CLC[1]. Based on the results listed in Table 4, both the reduction and gasification rates increased as temperatures increased but the rate increase was not linear with the temperature. The reduction rate was up 37% from 950°C to 1000°C and this was much higher than the rate increase (5.4%) from 1000°C to 1100°C. This was mainly due to the increased gasification rate from 950°C to 1000°C (44%) and was higher than the rate increase from 1000°C to 1100°C (11.1%). The reduction rates were slightly higher or similar to the gasification rates at all test temperatures because the reduction of the OC with

syngas (mainly CO+H_2) generated from gasification sped up the gasification reaction. The increasing gasification rate by the OC also resulted in a lower maximum temperature during reduction than char gasification (Table 4). During the test at 1100^{o}C, the maximum temperature Tmax=972^{o}C was below 1000^{o}C.

The CO_2 conversion efficiencies of reduction were higher than char gasification at the same temperature for all three test temperatures (Table 4). During reduction, the char was first gasified to syngas then the syngas (mainly CO and H_2) was oxidized to CO_2 and H_2O by the OC. The CO_2 conversion efficiencies of reduction at 1100^{o}C were lower than at 1000^{o}C and 950^{o}C (Table 4). For char gasification, the CO_2 conversion efficiencies decreased as temperature increased from 950 to 1100^{o}C, which indicated that more CO was in the syngas at high temperature. As the char gasification temperature increased, more CO was generated from the water gas reaction (R6) because this reaction is endothermic and thermodynamically favored at higher temperature. On the other hand, less CO was converted to CO_2 through the water gas shift reaction (R8) because the reaction is exothermic and thermodynamically favored at lower temperature. This resulted in more CO in the syngas from high temperature char gasification.CO is not desired in the product gas and may require an oxygen polishing step to be converted to CO_2. Therefore, the Fe40Cu20 OC in coal iG-CLC at temperature $\geq$ 1100^{o}C did not show any benefit based on the CO_2 conversion efficiency and the rate.

3.2.4. Impact of OC to char ratios (ϕ) on CO_2 conversion efficiency Sco_2 and OC phase changes

The Fe40Cu20 OC with char at different ratios ϕ= 24, 40 and 80 was tested at 1000^{o}C in Ar+H_2O. The final carbon conversion efficiencies, maximum conversion rates and temperatures were similar for all three tested ratios. The CO_2 conversion efficiencies reduced as the ratio of OC to char decreased (Table 5). The low Sco_2 indicated that there was more CO in the product gas,

but this was still higher than the char gasification results at the same condition (Sco_2=0.54) (Table 4 and 5). In addition, the higher H_2 concentrations in the product gas were related to the lower OC to char ratios (Figure 5). Compared to char gasification, the reductions at ϕ = 80, 40 and 24 converted 94%, 92% and 60% of H_2 produced from gasification, respectively. H_2 and CO in the product gas will require further treatment (such as oxygen polishing) to obtain high purity CO_2 for CO_2 sequestration.

Table 5. The CO_2 conversion efficiencies, the reduced Fe40Cu20 OC and Fe20Cu40 OC phase changes at different ratios of the OC to char ϕ in Ar+H_2O at 1000°C.

OC/char ϕ	Process (gas)	Sco_2	Reduced OC phase changes			
Fe40Cu20 OC			CuO	$CuFeO_2$	$Cu_xFe_{3-x}O_4$	Cu
80	IG-CLC (Ar+H_2O)	0.88	NA	major	major	trace
40		0.80	NA	minor/trace	major	minor
24		0.76	NA	NA	major	minor
Fe20Cu40 OC						
67	CLOU (Ar)	0.96	major	major	trace	NA
	CLOU (Ar+H_2O)	0.96	major	major	trace	NA
18	IG-CLC (Ar+H_2O)	0.76	NA	NA	major	major

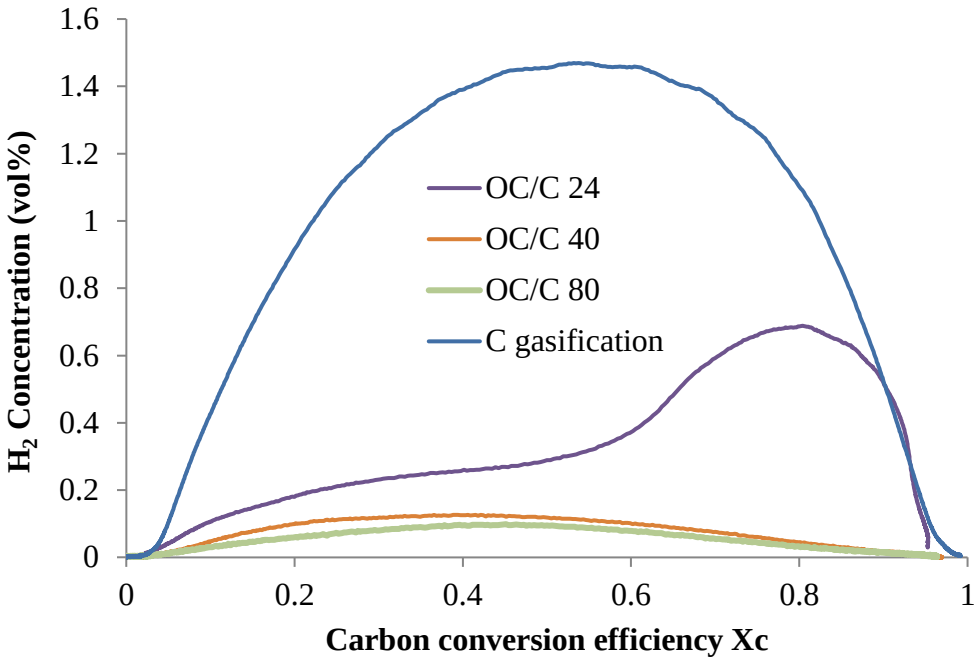

Figure 5. The H_2 concentrations vs carbon conversions for coal char reactions with Fe40Cu20 OC at ϕ = 80, 40 and 24 and coal char gasification with SiO_2 (same amount as the OC) at 1000°C in Ar+H_2O.

To understand the phase changes of active metal oxides in the OC during reduction with char, the residues of the reduced Fe40Cu20 OC at ϕ = 80, 40 and 24 were analyzed by XRD. For the Fe40Cu20 OC at ϕ = 80, $CuFeO_2$ (rhombohedral) (major) and $Cu_xFe_{3-x}O_4$ (x =0.67) (cubic) (major) with trace amounts of Cu were detected (Table 5). The trace Cu might be generated from the CuO in the fresh Fe40Cu20 OC. The residue of the Fe40Cu20 OC at ϕ = 40 had $CuFeO_2$ (rhombohedral) (minor or trace), $Cu_xFe_{3-x}O_4$ (x =0.67) (cubic) (major) and Cu (minor) (Table 5). Partial $CuFeO_2$ was further reduced to Cu and $Cu_xFe_{3-x}O_4$. For the OC at ϕ = 24, $Cu_xFe_{3-x}O_4$ (x =0.67) (cubic) (major) and Cu (minor) were present in the residue (Table 5). All of the $CuFeO_2$ was further reduced to Cu and $Cu_xFe_{3-x}O_4$. As ϕ decreased, the active metal oxides were further reduced and the phase changes were:

CuFe_2O_4 ($Cu_xFe_{3-x}O_4$ x=1 or $CuOFe_2O_3$) →

CuFeO_2($Cu_2OFe_2O_3$) + **Cu**$_xFe_{3-x}O_4$ (X=0.67 or 0.86) (ϕ = 80) →

CuFeO_2($Cu_2OFe_2O_3$) + **Cu**$_xFe_{3-x}O_4$ (X=0.67 or 0.86) + **Cu** (ϕ = 40) →

Cu$_xFe_{3-x}O_4$ (X=0.67 or 0.86) + **Cu** (ϕ = 24).

So, CuO in the $CuFe_2O_4$ was more active and easily reduced from CuO/Cu_2O/Cu compared to Fe_2O_3 from Fe_2O_3/Fe_3O_4/FeO/Fe. This was in agreement with the phase equilibrium in the system Cu-Fe-O at 1000^{o}C as a function of oxygen partial pressure [30, 31]. As the oxygen partial pressure decreased (Log P_{O2} 0 to -15), the phases in the Fe40Cu20 OC, with $n_{Fe}/(n_{Fe}+n_{Cu})$ = 0.67 were:

$Cu_xFe_{3-x}O_4/CuFeO_2$ + $Cu_xFe_{3-x}O_4/Cu_xFe_{3-x}O_4$ + Cu/ FeO + Cu/Fe + Cu.

Therefore, reducing Fe_2O_3 to FeO and Fe were more difficult compare to CuO to Cu. So, for the Cu-Fe OC in iG-CLC, the optimum ratio of OC to coal is important to avoid agglomeration caused by Cu at high temperature.

3.3. Fe20Cu40 OC with Coal Char in CLOU

3.3.1. Reactivity of Fe20Cu40 OC and coal char with ϕ 67 at 1000^{o}C in Ar

The reactivity of the OC with the coal char was tested at 1000^{o}C in Ar. The final carbon conversion efficiency of char was Xc=1.0 at 1000°C. This was close to the theoretical carbon conversion efficiency (1) and indicated that the chars were completely converted. Based on the oxygen transport capacity, Ro = 0.04 g O_2/g OC (Table 4), 670 mg of Fe20Cu40 OC releases 26.8 mg gaseous O_2 that ideally combusts 10.05 mg carbon, which is more carbon than present in the char (8.46 mg). Therefore, the char should be completely combusted by the O_2 released from the Fe20Cu40 OC and generate mainly CO_2 and a small amount of O_2 in the product gas.

The QMS detected mainly CO_2 with small amounts of O_2 and CO in the product gases during the test (Figure 6). The O_2 was mainly generated at the end of the test (temperatures above

949°C, Xc > 0.8) as expected less carbon and excess O_2 in the system. Little CO was produced at the beginning of the test because the released O_2 was relatively small at the lower temperature and

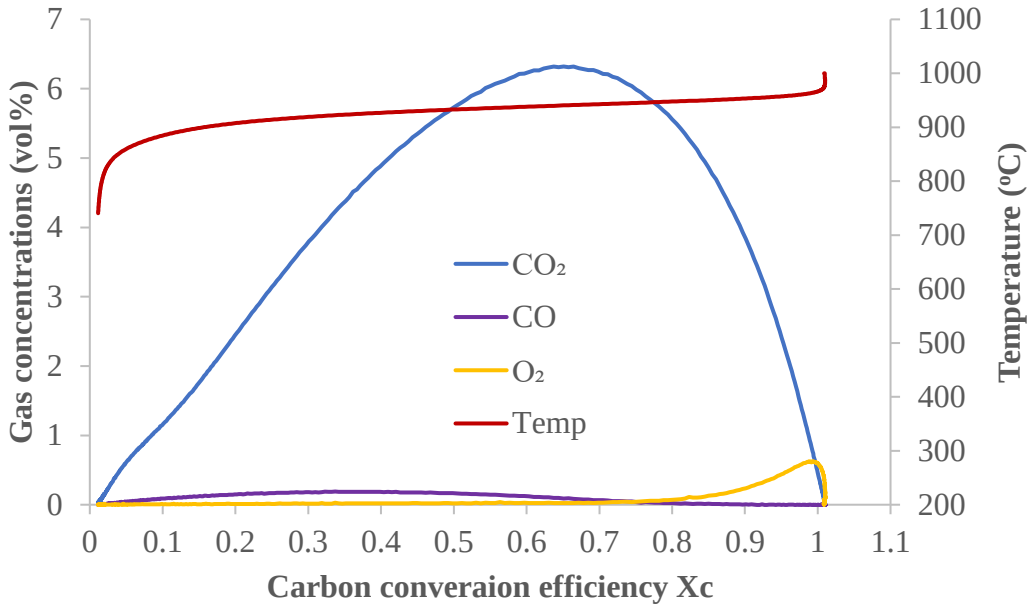

Figure 6. The gas concentrations vs carbon conversion efficiencies of the coal char reactions with Fe20Cu40 OC/char ratios ϕ = 67 at 1000°C in Ar.

carbon partial oxidation took place. Therefore, Fe20Cu40 OC uncoupling and char combustion were the main reactions and char partial combustion was a minor reaction. The reactions were further supported by XRD phase analysis of the residues of reduced Fe20Cu40 OC with char. CuO and $CuFe_2O_4$ in the Fe20Cu40 OC were reduced to Cu_2O and $CuFeO_2$ ($Cu_2OFe_2O_3$) respectively, which was the same as the Fe20Cu40 OC oxygen uncoupling. In addition, after re-oxidation of the reduced Fe20Cu40 OC in 22.4% O2/Ar, the phases were CuO and $CuFe_2O_4$ (tetragonal, cubic) and were the same as the fresh Fe20Cu40 OC (Table 2). So, after one cycle, the Fe20Cu40 OC did not change its phases and may be used for multi-cycle testing in the future.

The carbon conversion rate had a maximum dXc/dt = 0.0083 s^{-1} at Tmax = 942°C. This was lower than the carbon conversion rate of pure CuO with char at ϕ=26 and 950 °C, dXc/dt =

0.012 s^{-1} [19]. It is due to lower uncoupling rate of the Fe20Cu40 OC compared to CuO (Table 3). The maximum reduction rate of the Fe20Cu40 OC with char was slightly faster than the oxygen uncoupling rate of Fe20Cu40 OC. It also occurred at a lower temperature Tmax than the Fe20Cu40 OC oxygen uncoupling Tmax (Table 3). This was because the oxygen generated from uncoupling was consumed by the char and the char combustion increased the rate of oxygen uncoupling. Compared to the Fe40Cu20 OC with char in iG-CLC at 1000^{o}C (Table 4), the carbon conversion rate of Fe20Cu40 OC with char in CLOU was about two times faster. In addition, the CO_2 conversion efficiency of the Fe20Cu40 OC in CLOU (Sco_2=0.97) was higher than the Fe40Cu20 OC in iG-CLC (Sco_2=0.88) (Table 5).

3.3.2. Impact of water on the Fe20Cu40 OC and Coal Char Reactions

The Fe20Cu40 OC with char at ϕ = 67 was also tested at 1000^{o}C in Ar+H_2O to study the impact of water on its reactivity. The carbon conversion efficiency Xc=0.98 was similar to the test at the same ϕ in Ar. There was a slight difference in the carbon conversion rate and compositions of the product gas between in Ar+H_2O and Ar. In Ar+H_2O, the maximum rate $dXc/dt=0.0088s^{-1}$ at Tmax=938 ^{o}C was slightly higher due to char gasification and syngas combustion by O_2 released from the OC along with the char combustion with O_2. Syngas combustion is usually faster than direct char combustion. H_2 was detected along with CO but the amount of CO was smaller compared to the test with Ar only. This may have occurred due to the water gas shift reaction at relatively low temperatures as the sample heated to the test temperature. The XRD phase analysis results of the reduced Fe20Cu40 OC residue with char in Ar+H_2O were the same as the test in Ar. Therefore, Fe20Cu40 OC uncoupling and char combustion were the main reactions for the Fe20Cu40 OC with char at ϕ = 67 in Ar+H_2O. Additional char gasification and syngas combustion were minor reactions.

3.3.3. Impact of the Fe20Cu40 OC to char ratio on reactivity and the OC phase changes

The Fe20Cu40 OC with char at $\phi = 18$ was tested at 1000°C in Ar+H_2O to study the impact of Fe20Cu40 OC to char ratio on reactivity and the OC phase changes. The final carbon conversion efficiency, maximum rate and CO_2 conversion efficiency were Xc=0.97, $dXc/dt=0.0031s^{-1}$ at Tmax = 960°C, and Sco_2=0.76, respectively. The reaction generated mainly CO_2 with small amounts of CO and H_2 (Figure 7). The remaining sample contained Cu and $Cu_xFe_{3-x}O_4$ (X=0.67) from XRD analysis (Table 5). These reactivity results were different than the test of Fe20Cu40 OC with char at $\phi = 67$ in Ar and Ar+H_2O (CLOU) but similar to the test of Fe40Cu20 OC and char at $\phi = 24$ in Ar+H_2O (IG-CLC). Based on the oxygen transport capacity of the Fe20Cu40 OC from oxygen uncoupling (Ro = 0.04) (Table 3), the released O_2 ideally combusts 32% of the char to CO_2 at $\phi = 18$. Therefore, char gasification and syngas reduction took place with char combustion in the test with Fe20Cu40 OC and char. This was the same as iG-CLC and agreed with the reported study using pure CuO with char at $\phi = 8$, 850°C and 950°C in Ar+H_2O[19]. When pure CuO reacted with char in Ar at the same conditions, the carbon conversion efficiencies were Xc = 0.34 at 850°C and 0.67 at 950°C[19]. This indicated that the carbon was not completely converted. This was also the reason that Fe20Cu40 OC with char at $\phi = 18$ in Ar was not tested. To achieve a high CO_2 conversion efficiency with CLOU, selecting a suitable ratio of OC to coal is necessary.

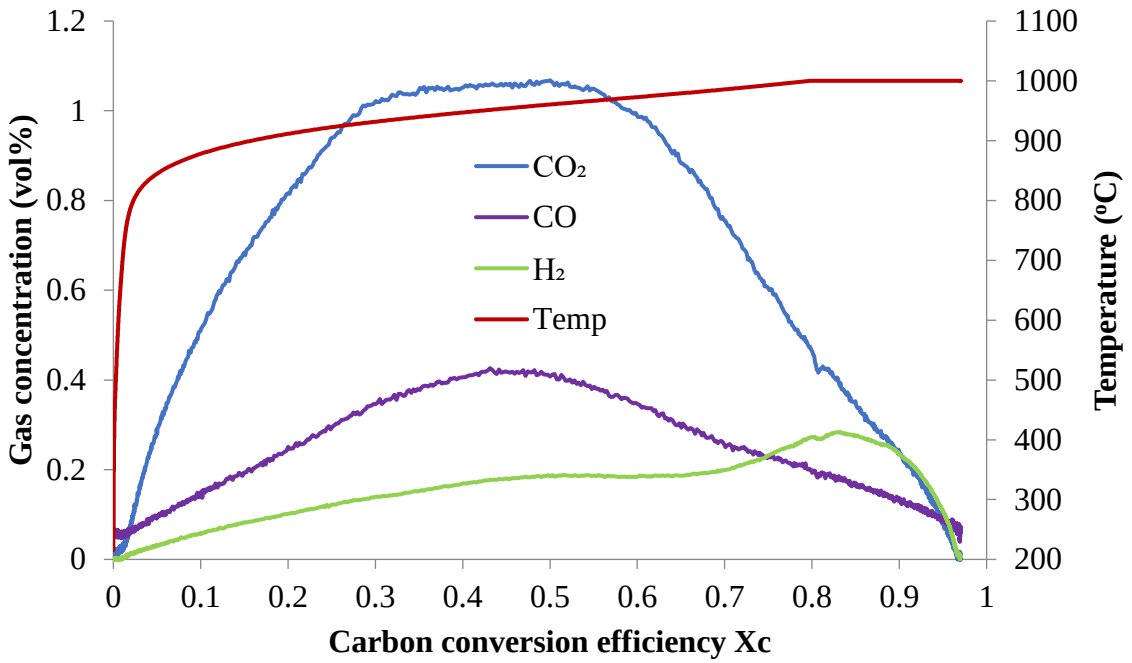

Figure 7. The gas concentrations vs carbon conversion efficiencies of the coal char reactions with Fe20Cu40 OC/char ratio ϕ = 18 at 1000°C in Ar+H_2O.

4. Conclusions

Bimetallic Cu-Fe oxygen carriers (OC) with SiO_2 as a support (Cu-Fe-Si) have the potential for low cost since they can be derived from naturally occurring materials. Two Cu-Fe OCs: 40% Fe_2O_3+20%CuO+40%SiO2 (by weight) (Fe40Cu20) and 40%CuO+20%Fe_2O_3+40%SiO2 (by weight) (Fe20Cu40) were prepared using a pressure pelletizing method. From XRD analysis, the Fe40Cu20 OC contained mostly $CuFe_2O_4$, but the Fe20Cu40 OC had mostly CuO along with $CuFe_2O_4$. During the preparation, CuO and Fe_2O_3 reacted and formed $CuFe_2O_4$ ($CuOFe_2O_3$). Both the Fe40Cu20 and Fe20Cu40 OCs released gaseous O_2, but the uncoupling rate of the Fe20Cu40 OC was 2.5 times higher than the Fe40Cu20 OC.

Reactivities of the prepared Cu-Fe OCs were investigated at high temperatures in coal iG-CLC and CLOU. For the Fe40Cu20 OC in coal char iG-CLC with a ratio of OC to char ϕ = 80 at 950°C, 1000°C and 1100°C in Ar+H_2O, the reduction rate increased by 37% from 950°C to 1000°C. This was much higher than the rate increase (5.4%) from 1000°C to 1100°C due to the char gasification rate increasing. The CO_2 conversion efficiency at 1100°C was lower than at 1000°C and 950°C. Therefore, the Fe40Cu20 OC in coal iG-CLC at temperatures ≥ 1100°C did not have an obvious benefit. The addition of CuO in monometallic Fe-based OC improved the CO_2 conversion efficiency Sco_2 compared to the Fe-based OC at the highest Sco_2 (Fe_2O_3 to Fe_3O_4 and excess OC needed). To achieve this advantage, the optimum ratio of OC to coal (like ϕ= 80) is important to avoid agglomeration caused by Cu at high temperature. The contents of Cu in the reduced Fe40Cu20 OC increased as the ratio of OC to char descended from ϕ= 80, 40 and 24. This maybe be a result of easily reduced Cu oxides compared to Fe oxides. In addition, the CO_2 conversion efficiencies reduced as the ratio decreased.

For the Fe20Cu40 OC in coal char CLOU with ϕ = 67 tested with Ar+H_2O, the primary reactions and reactivities were similar to those with Ar. As the ratio of OC to char decreased ϕ = 18, the reactions and reactivities were similar to iG-CLC with Fe40Cu20 OC and char at ϕ = 24 in Ar+H_2O. At lower ϕ = 18, Cu was generated and may cause agglomeration at high temperature. To prevent this, the optimum ratio of OC to coal in CLOU is very important, especially in a coal gasification gas environment (e.g. steam).

For the Fe40Cu20 OC in coal iG-CLC with ϕ = 80 at 1000°C, the carbon conversion rate was $dXc/dt=0.0037\ s^{-1}$ and CO_2 conversion efficiency Sco_2=0.88. The carbon conversion rate of Fe20Cu40 OC in coal CLOU with ϕ = 67 was $dXc/dt=0.0083\ s^{-1}$ and about two times faster than the Fe40Cu20 OC in coal iG-CLC. In addition, the CO_2 conversion efficiency of the Fe20Cu40

OC was Sco_2=0.96 and higher than the Fe40Cu20 OC. Overall, Cu-Fe-Si has potential as a competitive oxygen carrier in the high temperature coal chemical looping combustion process.

ACKNOWLEDGMENTS

This report was prepared as an account of work sponsored by the Department of Energy, National Energy Technology Laboratory, an agency of the United States Government. Neither the United States Government nor any agency thereof, nor any of their employees, makes any warranty, expressed or implied, or assumes any legal liability or responsibility for the accuracy, completeness, or usefulness of any information, apparatus, product, or process disclosed, or represents that its use would not infringe privately owned rights. Reference herein to any specific commercial product, process, or service by trade name, trademark, manufacturer, or otherwise, does not necessarily constitute or imply its endorsement, recommendation, or favoring by the United States Government or any agency thereof. The views and opinions of authors expressed herein do not necessarily state or reflect those of the United States Government or any agency thereof.

REFERENCES

[1] Wang P, Means N, Shekhawat D, Berry D, Massoudi M. Chemical-Looping Combustion and Gasification of Coals and Oxygen Carrier Development: A Brief Review. Energies. 2015;8:10605-35.
[2] Adanez J, Abad A, Mendiara T, Gayan P, de Diego LF, Garcia-Labiano F. Chemical looping combustion of solid fuels. Progress in Energy and Combustion Science. 2018;65:6-66.
[3] Adanez J, Abad A, Garcia-Labiano F, Gayan P, de Diego LF. Progress in Chemical-Looping Combustion and Reforming Technologies. Progress in Energy and Combustion Science. 2012;38:215-82.
[4] Ströhle J, Orth M, Epple B. Design and operation of a 1 MWth chemical looping plant. Applied Energy. 2014;113:1490-5.
[5] Ohlemüller P, Ströhle J, Epple B. Chemical looping combustion of hard coal and torrefied biomass in a 1 MWth pilot plant. International Journal of Greenhouse Gas Control. 2017;65:149-59.
[6] Ströhle J, Orth M, Epple B. Chemical looping combustion of hard coal in a 1 MWth pilot plant using ilmenite as oxygen carrier. Applied energy. 2015;157:288-94.
[7] Flynn TJ, Velazquez-Vargas, Luis G., Bao, Jinhua, Zhang, Yitao, Tong, Andrew, and Fan, Liang-Shih. 250 kWt Pilot Testing in Support of a 10 MWe Coal-Direct Chemical Looping Demonstration Feasibility Study. 2019 Clean Energy Conference. Clearwater, Florida: https://www.osti.gov/servlets/purl/1542914; 2019.
[8] Bayham S, McGiveron O, Tong A, Chung E, Kathe M, Wang D, et al. Parametric and dynamic studies of an iron-based 25-kW(th) coal direct chemical looping unit using sub-bituminous coal. Applied Energy. 2015;145:354-63.
[9] Tong A, Bayham S, Kathe MV, Zeng L, Luo S, Fan L-S. Iron-based syngas chemical looping process and coal-direct chemical looping process development at Ohio State University. Applied Energy. 2014;113:1836-45.
[10] Tong A, Kathe MV, Wang D, Fan LS. The Moving Bed Fuel Reactor Process. In: Breault RW, editor. In Handbook of Chemical Looping Technology: Wiley; 2018.
[11] Abad A, Adanez-Rubio I, Gayan P, Garcia-Labiano F, de Diego LF, Adanez J. Demonstration of chemical-looping with oxygen uncoupling (CLOU) process in a 1.5 kW(th) continuously operating unit using a Cu-based oxygen-carrier. International Journal of Greenhouse Gas Control. 2012;6:189-200.

[12] Adanez-Rubio I, Abad A, Gayan P, de Diego LF, Garcia-Labiano F, Adanez J. Performance of CLOU process in the combustion of different types of coal with CO2 capture. International Journal of Greenhouse Gas Control. 2013;12:430-40.
[13] Adánez-Rubio I, Abad A, Gayán P, García-Labiano F, Luis F, Adánez J. Coal combustion with a spray granulated Cu-Mn mixed oxide for the Chemical Looping with Oxygen Uncoupling (CLOU) process. Applied energy. 2017;208:561-70.
[14] Pérez-Vega R, Adánez-Rubio I, Gayán P, Izquierdo MT, Abad A, García-Labiano F, et al. Sulphur, nitrogen and mercury emissions from coal combustion with CO2 capture in chemical looping with oxygen uncoupling (CLOU). International Journal of Greenhouse Gas Control. 2016;46:28-38.
[15] Mattisson T, Lyngfelt A, Leion H. Chemical-looping with oxygen uncoupling for combustion of solid fuels. International Journal of Greenhouse Gas Control. 2009;3:11-9.
[16] Adanez-Rubio I, Arjmand M, Leion H, Gayan P, Abad A, Mattisson T, et al. Investigation of Combined Supports for Cu-Based Oxygen Carriers for Chemical-Looping with Oxygen Uncoupling (CLOU). Energy & Fuels. 2013;27:3918-27.
[17] Adanez-Rubio I, Gayan P, Abad A, de Diego LF, Garcia-Labiano F, Adanez J. Evaluation of a Spray-Dried CuO/MgAl2O4 Oxygen Carrier for the Chemical Looping with Oxygen Uncoupling Process. Energy & Fuels. 2012;26:3069-81.
[18] Adanez J, Abad A. Chemical-looping combustion: Status and research needs. Proceedings of the Combustion Institute. 2019;37:4303-17.
[19] Wang P, Means N, Howard BH, Shekhawat D, Berry D. The reactivity of CuO oxygen carrier and coal in Chemical-Looping with Oxygen Uncoupled (CLOU) and In-situ Gasification Chemical-Looping Combustion (iG-CLC). Fuel. 2018;217:642-9.
[20] Jiang SX, Shen LH, Wu J, Yan JC, Song T. The investigations of hematite-CuO oxygen carrier in chemical looping combustion. Chemical Engineering Journal. 2017;317:132-42.
[21] Yang W, Zhao H, Ma J, Mei D, Zheng C. Copper-Decorated Hematite as an Oxygen Carrier for in Situ Gasification Chemical Looping Combustion of Coal. Energy & Fuels. 2014;28:3970-81.
[22] Siriwardane R, Tian HJ, Simonyi T, Poston J. Synergetic effects of mixed copper-iron oxides oxygen carriers in chemical looping combustion. Fuel. 2013;108:319-33.
[23] Gauthier T, Yazdanpanah M, Forret A, Amblard B, Lambert A, Bertholin S. CLC, a promising concept with challenging development issues. Powder Technology. 2017;316:3-17.
[24] Wang P, Howard B, Means N, Shekhawat D, Berry D. Coal Chemical-Looping with Oxygen Uncoupling (CLOU) Using a Cu-Based Oxygen Carrier Derived from Natural Minerals. Energies. 2019;12:1453.
[25] Chuang SY, Dennis JS, Hayhurst AN, Scott SA. Development and performance of Cu-based oxygen carriers for chemical-looping combustion. Combustion and Flame. 2008;154:109-21.
[26] Tian X, Zhao HB, Ma JC. Cement bonded fine hematite and copper ore particles as oxygen carrier in chemical looping combustion. Applied Energy. 2017;204:242-53.
[27] Gayan P, Adanez-Rubio I, Abad A, de Diego LF, Garcia-Labiano F, Adanez J. Development of Cu-based oxygen carriers for Chemical-Looping with Oxygen Uncoupling (CLOU) process. Fuel. 2012;96:226-38.
[28] Adanez J, de Diego LF, Garcia-Labiano F, Gayan P, Abad A, Palacios JM. Selection of oxygen carriers for chemical-looping combustion. Energy & Fuels. 2004;18:371-7.
[29] Bhavsar S, Tackett B, Veser G. Evaluation of iron- and manganese-based mono- and mixed-metallic oxygen carriers for chemical looping combustion. Fuel. 2014;136:268-79.
[30] Katkov AE, Lykasov AA. Spinel phase relations in the Fe3O4-CuFe2O4 system. Inorganic Materials. 2003;39:171-4.

[31] Jacob K, Fitzner K, Alcock C. Activities in the spinel solid solution, phase equilibria and thermodynamic properties of ternary phases in the system Cu-Fe-0. Metallurgical Transactions B. 1977;8:451-60.
[32] Ristic M, Hannoyer B, Popovic S, Music S, Bajraktaraj N. Ferritization of copper ions in the Cu-Fe-O system. Materials Science and Engineering B-Solid State Materials for Advanced Technology. 2000;77:73-82.
[33] Zhao HB, Wang K, Fang YF, Ma JC, Mei DF, Zheng CG. Characterization of natural copper ore as oxygen carrier in chemical-looping with oxygen uncoupling of anthracite. International Journal of Greenhouse Gas Control. 2014;22:154-64.
[34] Wang B, Yan R, Zhao H, Zheng Y, Liu Z, Zheng C. Investigation of Chemical Looping Combustion of Coal with CuFe2O4 Oxygen Carrier. Energy & Fuels. 2011;25:3344-54.
[35] Khvan AV, Fabrichnaya OB, Savinykh G, Adam R, Seifert HJ. Thermodynamic Assessment of the Cu-Fe-O System. J Phase Equilib Diffus. 2011;32:498-511.
[36] Higman C, and van der Burgt, M Gasification. 2nd ed. New York: Elsevier; 2008.
[37] Jerndal E, Mattisson T, Lyngfelt A. Thermal analysis of chemical-looping combustion. Chemical Engineering Research & Design. 2006;84:795-806.
[38] Chen H, Zheng Z, Chen Z, Bi XT. Reduction of hematite (Fe2O3) to metallic iron (Fe) by CO in a micro fluidized bed reaction analyzer: A multistep kinetics study. Powder technology. 2017;316:410-20.